

Prediction of storm surge on evolving landscapes under climate change

Mohammad Ahmadi¹, David R Johnson^{1,2}

¹ School of Industrial Engineering, Purdue University, West Lafayette, IN

² Department of Political Science, Purdue University, West Lafayette, IN

Abstract

Planners who wish to manage coastal flood risk with long-lived infrastructure (e.g., levees, floodwalls) under a constrained computational budget face a tradeoff. Simulating a large number of future time periods or scenarios with different assumptions about land subsidence, sea level rise, land accretion, imposes a limit on how many storm simulations can be run in each scenario and time period. Machine learning approaches have been developed to reduce the computational burden of predicting storm surge from many tropical cyclone events, but prior efforts focus on predicting surge as a function of storm parameters on a single landscape. In this analysis, we present a deep learning model that also incorporates landscape characteristics and boundary conditions (e.g., mean sea level). The model is informed by a dataset of peak surge elevations from Advanced Circulation (ADCIRC) hydrodynamic simulations of coastal Louisiana in eleven scenarios: a 2020 baseline and decadal time slices from 2030 to 2070 under two scenarios varying land subsidence and sea level rise rates. Training on ten scenarios to make predictions on the eleventh yields a grand RMSE of 0.086 m and grand MAE of 0.050 m over 90 storms per scenario and over 94,000 geospatial locations. We also aggregated the 90 storms in each scenario to generate an annual exceedance probability distribution; a two-sided Kolmogorov-Smirnov test comparing AEP estimates from the model predictions to the original ADCIRC simulations rejected the null hypothesis that the predictions and ADCIRC AEP values were drawn from the same distribution only 1.1% of the time.

Keywords

Storm surge, surrogate modeling, flood risk, landscape morphology, climate change

Introduction

Storm surge, the temporary increase in sea level caused by severe storms, is one of the most destructive components of tropical cyclones (TC), motivating the development of accurate tools and models for its prediction (Jia et al., 2015). In recent decades, high-fidelity numerical models have been produced that are able to estimate storm surge generated by tropical cyclone wind fields with high accuracy. However, these hydrodynamic simulations typically are computationally intense, requiring high-performance computing resources, and still there can be considerable biases in their outcome (J. Zhang et al., 2018).

Because physically-based models (i.e., solving fluid dynamics equations) like the ADvanced CIRCulation (ADCIRC) model (Luettich et al., 1992) can be very expensive in terms of

computational cost, surrogate models have been developed to predict storm surge without incurring the same high computational cost (Kyprioti, Taflanidis, Nadal-Caraballo, et al., 2021). The use of surrogate models or meta-models has increased rapidly in the field of coastal flood hazard research (Kyprioti et al., 2022). Surrogate models are useful tools in different fields because of their ability to emulate the behavior of complex models in their quest to approximate complex systems. Moreover, their computational efficiency makes them a convenient approach for tasks like optimization or modeling large ensembles of events and scenarios (Bartz-Beielstein & Zaefferer, 2017; Bekasiewicz et al., 2015).

Risk assessments, using techniques like joint probability methods to estimate a hazard curve, require simulation of a large number of synthetic storm events (i.e., thousands or tens of thousands). Computational limitations motivated advances such as the joint probability method with optimal sampling (JPM-OS) (Resio, 2007; Resio et al., 2009; Toro et al., 2010; Yang et al., 2019) and the use of heuristic algorithms to further reduce the number of simulations required for probabilistic flood risk (Fischbach et al., 2016; J. Zhang et al., 2018).

However, these approaches have limits, and consequently, planning studies still face meaningful constraints imposed by computational budgets. When evaluating the benefits of risk reduction infrastructure with long useful life spans, it is indeed important to consider risk and risk reduction over long planning horizons. Protection systems (e.g., levees, dikes, seawalls, pumping stations) must be designed to withstand and mitigate the effects of extreme events over many decades. This increases the necessity to consider uncertainties in factors that, over time, reshape the coastal landscape (e.g., land subsidence, land-use change, impacts of saltwater intrusion on vegetation) and boundary conditions (e.g., sea level rise) that determine risk to coastal communities; scenario analyses examine multiple future states of the world with different realizations of uncertain parameters. Integrated coastal management plans like Louisiana's *Comprehensive Master Plan for a Sustainable Coast* (Coastal Master Plan) evaluate the performance of a range of flood protection and coastal restoration projects implemented in different sequences, necessitating the modeling of multiple future time periods (Coastal Protection and Restoration Authority, 2023). Mokrech et al. (2011) stresses the importance of developing an integrated framework to assess long-term coastal impacts and thus make rational management decisions. Wamsley et al. (2009) investigated the storm surge and wave reduction benefits of different environmental restoration features (e.g., marsh restoration and barrier island changes), as well as the impact of future wetland degradation on local conditions, concluding that "consideration of natural features is required" to properly assess flood risk.

Studies that include multiple future time periods, states of the world, and project portfolios must evaluate risk on a large number of landscapes, and simple math dictates that under a fixed computational budget, the more landscapes planners want to model, the fewer events can be simulated per landscape. Using a lower-resolution mesh or a model simulating fewer physical processes may be an undesirable solution if it would introduce unacceptable biases and/or

uncertainty in storm surge estimates or compromise the ability of the model to resolve the impact of protection features like levees.

In this paper, we introduce a surrogate model using artificial neural networks (ANN) that can be used to resolve this computational constraint. We train the model on synthetic storms simulated on multiple landscapes using the ADCIRC model, including not only the storm parameters as features, but also landscape features (e.g., topographic/bathymetric elevations, canopy) and boundary conditions (e.g., mean sea level). We evaluate the accuracy to predict peak storm surge elevations, as well as the accuracy of annual exceedance probability (AEP) distributions estimated using the predicted surge values, finding that the model is sufficiently accurate for use as a scenario generator in planning studies.

Prior use of surrogate modeling for storm surge prediction

Previous studies have taken various approaches to applying surrogate models for prediction of storm surge and waves. Commonly, this means predicting peak storm surge elevations and peak significant wave heights at many points on a spatial grid as a function of the storm's characteristics at landfall. Studies vary in their choice of geography and TC characteristics, with the latter typically including parameters such as landfall location, angle of landfall, central pressure, forward velocity, radius of maximum windspeed, Holland-B parameter and/or tide level. Techniques for the surrogate models include kriging (Kyprioti, Taflanidis, Plumlee, et al., 2021; J. Zhang et al., 2018), kriging combined with principle component analysis (Jia et al., 2016; Jia & Taflanidis, 2013), support vector regression (Al Kajbaf & Bensi, 2020), and artificial neural networks (Chen et al., 2012). Al Kajbaf & Bensi (2020) provides a comparative assessment of the performance of these techniques.

Many other studies have focused on the use of surrogate models for forecasting future water surface elevations over the course of a storm (De Oliveira et al., 2009; Kim et al., 2019; Lee, 2006, 2009; Rajasekaran et al., 2008; Sztobryn, 2003). Recent works have incorporated sea level rise into predictions on a static landscape (Kyprioti, Taflanidis, Nadal-Caraballo, et al., 2021), but landscape morphology plays a significant role in modeling flood inundation and flood risk accurately (Bates et al., 2010). In areas exhibiting substantial land subsidence, erosion, barrier island migration, and other phenomena impacting morphology, incorporating sea level rise is necessary but insufficient for projecting future storm surges and inundation risks. Canopy and vegetation impact wind attenuation and surface friction, as shown in studies of mangrove forests and coastal wetlands on the Gulf coast of south Florida (K. Zhang et al., 2012). Mangrove forests reduced storm inundation areas and restricted surge inundation within a Category 3 hurricane zone, according to the study, finding that the width of the mangrove zone had a nonlinear effect on reducing surge amplitudes.

Although these previous studies investigated storm surge surrogate modeling from other perspectives, the impact of the combination of sea level rise (SLR), landscape and TC parameters on storm surge has not been thoroughly investigated. In this study, we aim to fill that gap by

developing a surrogate model using deep neural networks for the prediction of peak storm surge elevations from synthetic TCs as a function of their characteristics at landfall in coastal Louisiana, four landscape parameters impacting storm surge, and mean sea level.

Data

The synthetic tropical cyclones used in this study are characterized by their overall tracks and five parameters at landfall: forward velocity, radius of maximum windspeed, central pressure, landfall coordinates, and heading. The corpus of 645 synthetic storms was developed by the US Army Corps of Engineers for use in flood risk assessments based on the JPM-OS methodology (Nadal-Caraballo et al., 2020); each synthetic storm's landfall parameters serve as input data for the predictive model and are provided in Supplementary Information Table S1.

Hydrodynamic simulations from a coupled ADCIRC+SWAN model were available from Louisiana's 2023 Coastal Master Plan for all 645 synthetic storms, simulated on the plan's "Existing Conditions" landscape (i.e., 2020). A subset of 90 synthetic storms were simulated on each of 10 future landscapes representing decadal snapshots (i.e., 2030, 2040, 2050, 2060, 2070) under two different scenarios, a Lower and Higher Scenario, that vary in their assumptions about the rate of sea level rise, land subsidence, and other environmental factors (Coastal Protection and Restoration Authority, 2023; Cobell & Roberts, 2021). For each synthetic storm and landscape, peak storm surge elevations were extracted from the ADCIRC+SWAN simulations at 94,013 locations representing grid points from the Coastal Louisiana Risk Assessment model (CLARA) not located within fully-enclosed protection systems; the points form a mixed-resolution grid with a maximum 1-km spacing and higher resolution in some areas, such that every U.S. Census block contains at least one grid point (Johnson et al., 2023).

Each landscape is characterized by a digital elevation model defining the topography and bathymetry of the study region, as well as rasters defining other inputs to the ADCIRC model: the Manning's n value (i.e., bottom roughness coefficient), free surface roughness z_0 , and a surface canopy coefficient that captures the reduction in wind stress on water surfaces produced by local vegetation. All landscape characteristics were represented as GeoTIFFs with values extracted at each of the 94,013 grid point locations for use in the surrogate model. Full details regarding the Integrated Compartment Model used to develop the landscape representations are found in White et al. (2019) and Reed and White (2023), and details regarding the ADCIRC+SWAN model and Louisiana mesh are found in Cobell and Roberts (2021) and Roberts and Cobell (2017).

Methods

This study used feed-forward artificial neural network (ANN) models with multilayers and multiple outputs to predict storm surge at each location under current and future landscape conditions. A range of models varying from 128 neurons to 256 neurons was evaluated before selecting the models described here, as specifying too few neurons could impede the learning

process while using too many neurons could result in overtraining/overfitting (Jammoussi & Ben Nasr, 2020). Moreover, for all hidden layers, the RELU activation function was chosen with a learning rate of 0.001, and for the last layer, a linear activation function was selected to predict surge values. Using 100 epochs to train the model, the entire process was executed on an AMD Epyc 7662 CPU at 2.0 GHz, taking less than 7 hours for training to be completed in preparation for making predictions on a new landscape. For all folds in the cross-validation process, it took 70 hours. Once trained, less than 4 minutes is needed to generate predictions for a novel landscape.

Firstly, we examined the value of including landscape parameters in a predictive model of storm surge for a single landscape only. ANN models were trained for current conditions on 645 synthetic storms: a multi-layered feed-forward architecture with four hidden layers and an output layer of 1 dimension was used for predicting peak storm surge elevations at different locations. A “storm-only model” at each location only included the synthetic storm parameters at landfall as inputs. The “full model” included the synthetic storm parameters but also all grid points’ landscape parameters from the current landscape (latitudinal and longitudinal coordinates, topo/bathy NAVD88 elevation, surface canopy, z_0 , and Manning’s n). Sea level was excluded from the full model in this test because the local mean sea level was assumed constant throughout the study region, and thus only has variation when multiple landscapes are taken in as input data.

Next, to investigate the impacts of climate change and the slowly evolving landscape, we trained the full model using the 2020 landscape condition and 645 synthetic storms, as well as the 10 future landscapes, each with the same 90 synthetic storms. Predictive accuracy of the full model was evaluated utilizing leave-one-out cross-validation (LOOCV) on the future landscapes; in other words, for each fold of the CV procedure, the model was trained on the 2020 landscape and 9 of the 10 future landscapes, with predictions made on the tenth future landscape. We did this to reflect a real-world use case in which the full model could serve as a scenario generator, training on a set of landscapes run through ADCIRC and then predicting outcomes in novel landscapes. The current conditions landscape’s 645 storms were included to represent a realistic case in which a larger suite of synthetic TCs could be run on a single landscape as an input to a storm selection process that would identify the subset of 90 storms to run on other landscapes.

Finally, we also wanted to know how errors in the predicted peak storm surge from each synthetic storm propagate to differences in the estimated annual probability distribution of experiencing storm surge of varying elevations. This is ultimately what planners may care about when making decisions about flood protection projects. For this task, we employed the Coastal Louisiana Risk Assessment (CLARA) model, an implementation of JPM-OS which is the model used to estimate flood hazard for Louisiana’s Coastal Master Plan (Johnson et al., 2013, 2023). Full details on the CLARA model’s methodology are in Johnson et al. (2023); in this analysis, we compared peak surge elevation exceedance curves (i.e., surge elevations as a function of annual exceedance probability) generated from the simulated surge elevations from ADCIRC to exceedance curves

generated from the predicted surge elevations from the LOOCV procedure. The resulting empirical distributions were compared using a two-sample Kolmogorov-Smirnov (KS) test, which calculates the maximum difference between two empirical samples' cumulative distribution functions to test a null hypothesis that they have been drawn from the same underlying probability distribution function (Smirnov, 1939). CLARA produces estimates of surge exceedances at 23 return periods ranging from a 50% annual exceedance probability (AEP) to 0.005% AEP (i.e., the 2-year event to the 2,000-year event), so the two-sample KS test dictates that the null hypothesis be rejected at significance level α if

$$\sup_x |F_{ADCIRC}(x) - F_{ANN}(x)| > \sqrt{-\ln\left(\frac{\alpha}{2}\right) \cdot \frac{1}{23}}$$

where $F_{ADCIRC}(x)$ and $F_{ANN}(x)$ are the sample CDFs associated with the ADCIRC simulations and ANN predictions, respectively.

Results

The ANN model that includes landscape parameters performs markedly better than the model with only storm parameters when predicting surge from relatively intense storms, as shown for two illustrative storms in Figure 1. Each pane plots ADCIRC-simulated values against the ANN-predicted values at approximately 3,500 points on a west-to-east transect at 29.8° N, a latitude selected for its nearly continuous series of grid points uninterrupted by major water bodies or enclosed polders¹. Blue points represent the Full Model which includes landscape parameters, and red points represent the Storm-Only Model which excludes them. The left-hand pane shows Storm 495, a weaker TC with central pressure of 975 mb at landfall, while the right-hand pane shows the much stronger storm 11 with a landfalling central pressure of 905 mb.

Across all 645 synthetic storms and grid points in the current conditions landscape, the Storm-only Model reached an overall RMSE of 0.31 m, while the Full Model achieved an RMSE of 0.28 m (Table 1). While this does represent an improvement of over 10 percent, primarily the result of greater accuracy for larger surge elevations, we expected the difference between these models to be minimal when trained only on the current conditions landscape. This is because of the lack of variation in landscape parameters over the synthetic storms at each point and contrastingly greater variation in TC parameters.

¹ The sudden decrease in points with simulated surge below 0.36 NAVD88 m is due to this being the mean sea level assumed for the current conditions landscape. Grid points over water are initialized at this level, leaving very few points along the chosen transect with lower topographic elevation, typically due to being pumped and drained.

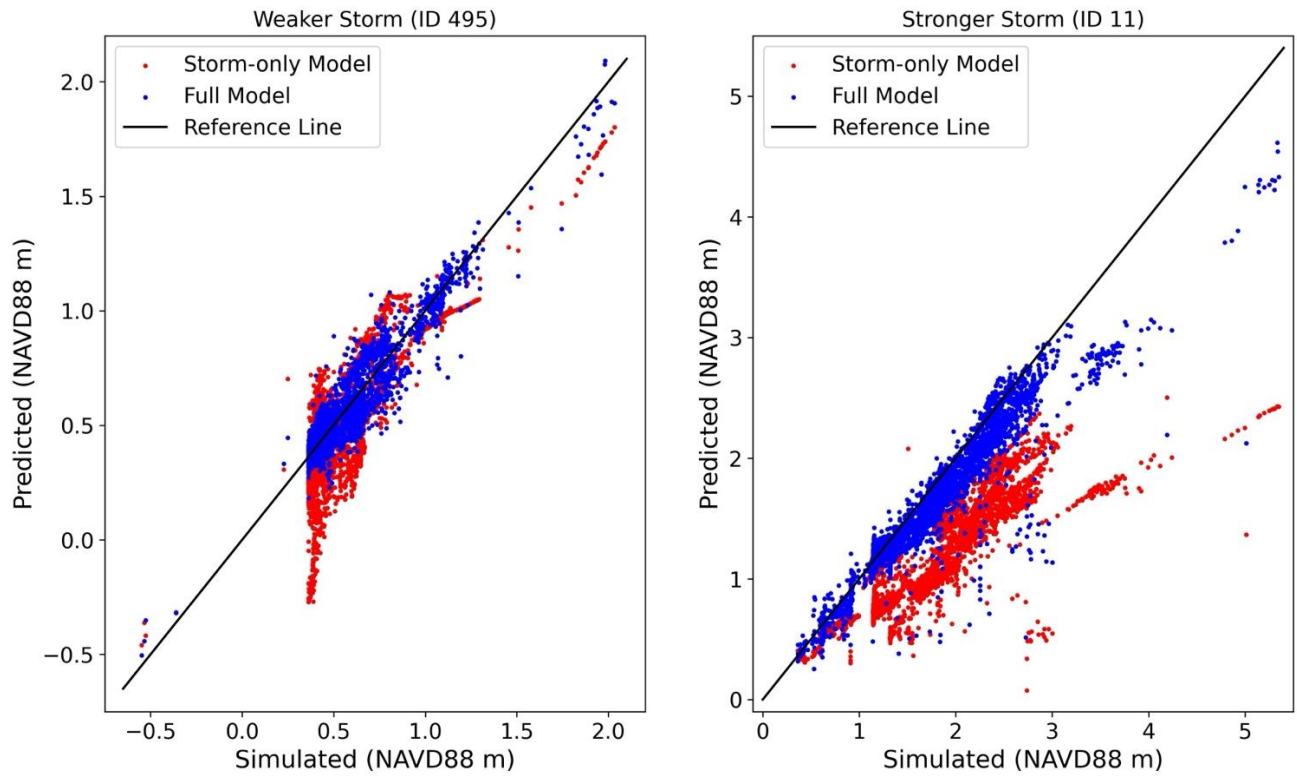


Figure 1. Simulated versus predicted storm surge for storm 495 (left pane) and storm 11 (right pane) in the cases where the ANN model input includes only storm parameters (red) and both storm and landscape parameters (blue) grid points along a transect at 29.8° N. *Note: Axis ranges vary between left and right panes.*

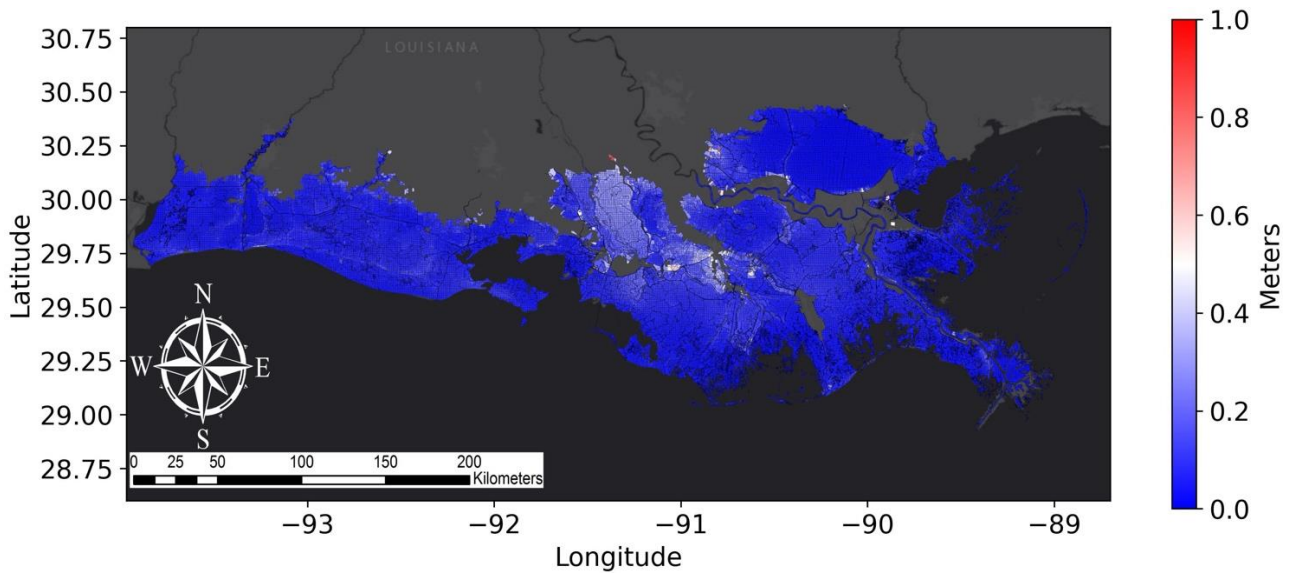


Figure 2. RMSE values across all landscapes and synthetic storms for all grid points in the study domain.

Examining the spatial pattern of the Full Model when trained on current and future scenarios, we see that points with higher RMSE over all storms and landscapes are generally further inland (Figure 2). This is expected, given that such points generally have fewer storms in the corpus that

produce wetting, and we did not employ any dry-node correction techniques like those used in Shisler & Johnson (2020) or Kyprioti, et al. (2021); instead, non-wetting observations were simply removed from the training set. The model also performed less accurately in areas with more complex hydrology, such as in unpopulated wetlands in the Atchafalaya River Basin (between 91° and 92° W longitude on the northern portion of the model domain), where the ADCIRC model also has greater uncertainty and bias when validated against historic TCs (Roberts & Cobell, 2017).

Considering the RMSE of the Full Model averaged over all landscapes and synthetic storms, the RMSE at 90% of grid points is less than 0.18 m, at 99% of grid points less than 0.38 m, and at 99.9% of grid points less than 0.79 m (Figure 3). Over the ten future scenarios used in the leave-one-landscape-out cross-validation procedure, the Full Model produced a grand RMSE of 0.086 m and grand mean absolute error (MAE) of 0.050 m (Table 1). These results compare favorably to the calibration and validation results from the ADCIRC+SWAN model used to generate the hydrodynamic simulations, which reported a standard error in simulated high-water marks of approximately 0.46 m over seven historical storms (hurricanes Katrina, Rita, Gustav, Ike, Isaac, Nate, and Harvey) (Cobell & Roberts, 2021). Further analysis incorporated into the 2023 Coastal Master Plan estimated an average standard error of 0.15 m in peak surge elevations over the grid cells included in this analysis (authors' own calculations).

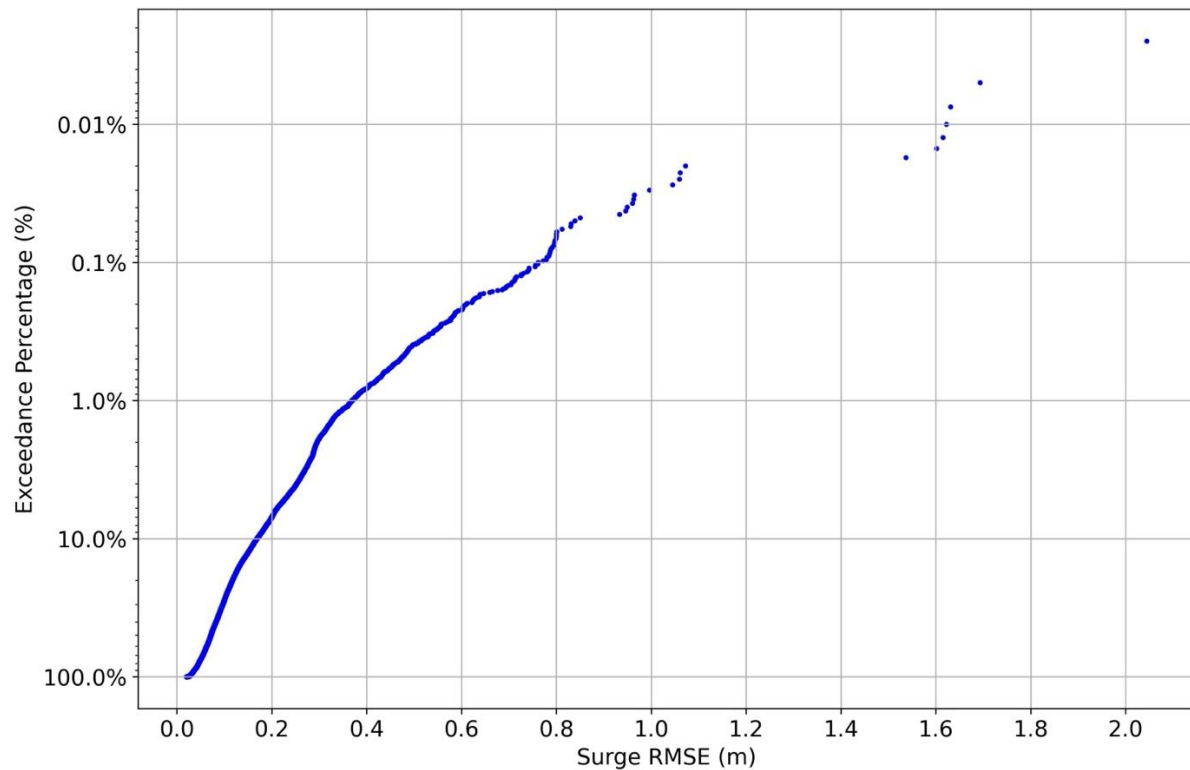


Figure 3. Exceedance percentage of RMSE values by grid point, with RMSE averaged across all landscapes and synthetic storms.

Figure 4 further disaggregates the model predictions to show the frequency distribution of predicted versus simulated surge elevations in each of the future landscapes over the synthetic storms and grid points. The overall distributions appear nearly indistinguishable except in the Higher Scenario’s 2070 landscape, the most extreme scenario with respect to its assumptions about mean sea level and cumulative land subsidence. That this scenario would be an outlier compared to the others is intuitive, given its more extreme assumptions about environmental conditions; in this sense, the 2070 Higher Scenario landscape is subject to the common difficulty of extrapolating beyond training data in the leave-one-landscape-out experimental design. That said, the directionality of the difference is somewhat counterintuitive. In this scenario, the predicted storm surge is on average greater than the simulated values, though the primary non-linear difference in the scenario is an accelerating rate of sea level rise. Despite this acceleration, it appears that the Full Model overestimates the gradient in storm surge associated with changes in mean sea levels.

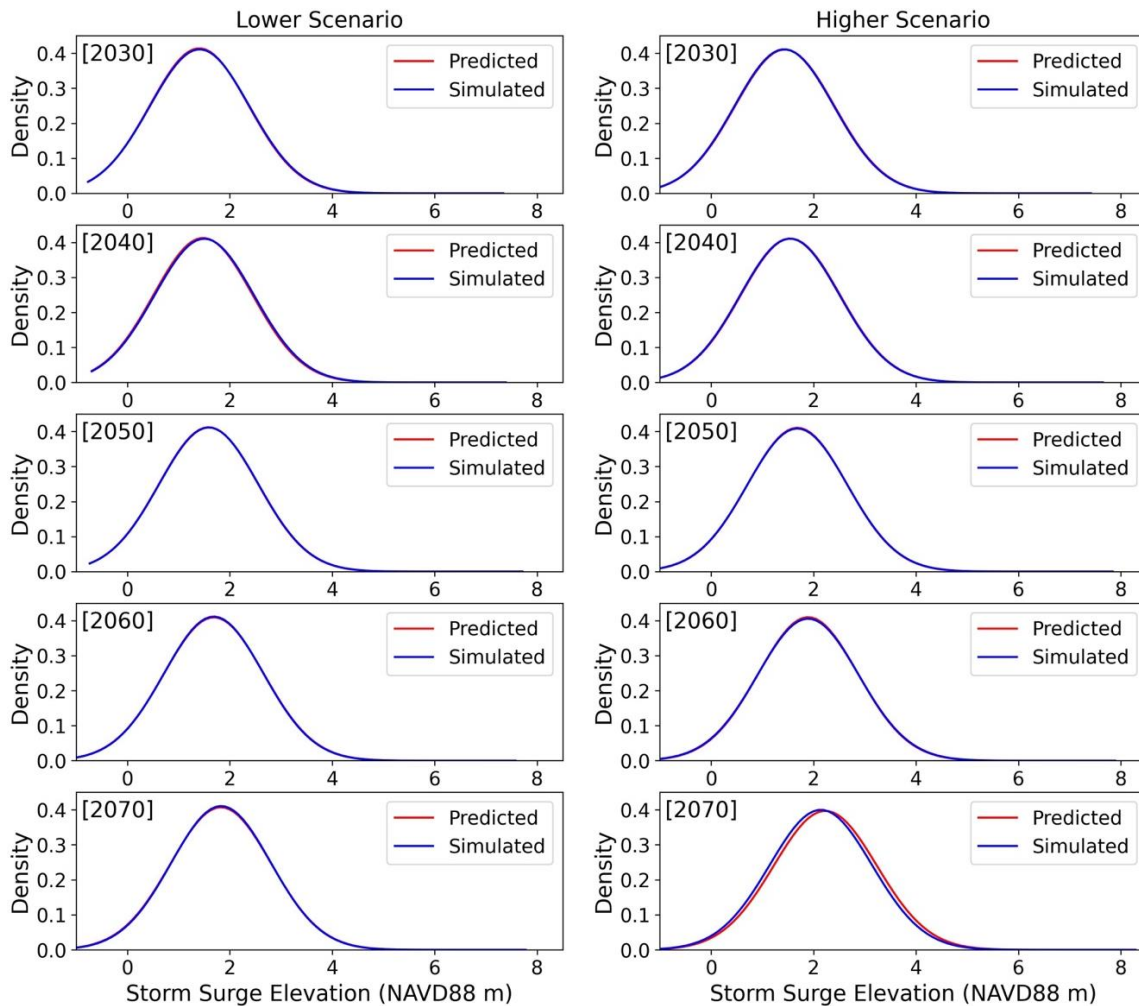


Figure 4. Frequency distribution of peak storm surge elevation (predicted versus simulated) for all future landscapes.

Examining the hazard aggregated over multiple TCs, the errors associated with surge predictions do not appear to meaningfully compound once aggregated to annual exceedance probability

curves, in the sense that the RMSEs over all grid points at a range of return periods are in a similar range to the RMSEs over all grid points and synthetic storms (between 0.05 and 0.1 m for all landscapes but the most extreme, as shown in Figure 5). The RMSE generally is larger at lower AEPs, consistent with an intuition that prediction is more challenging for extreme events associated with storm surge values near the upper bounds of observations in the simulated training sets.

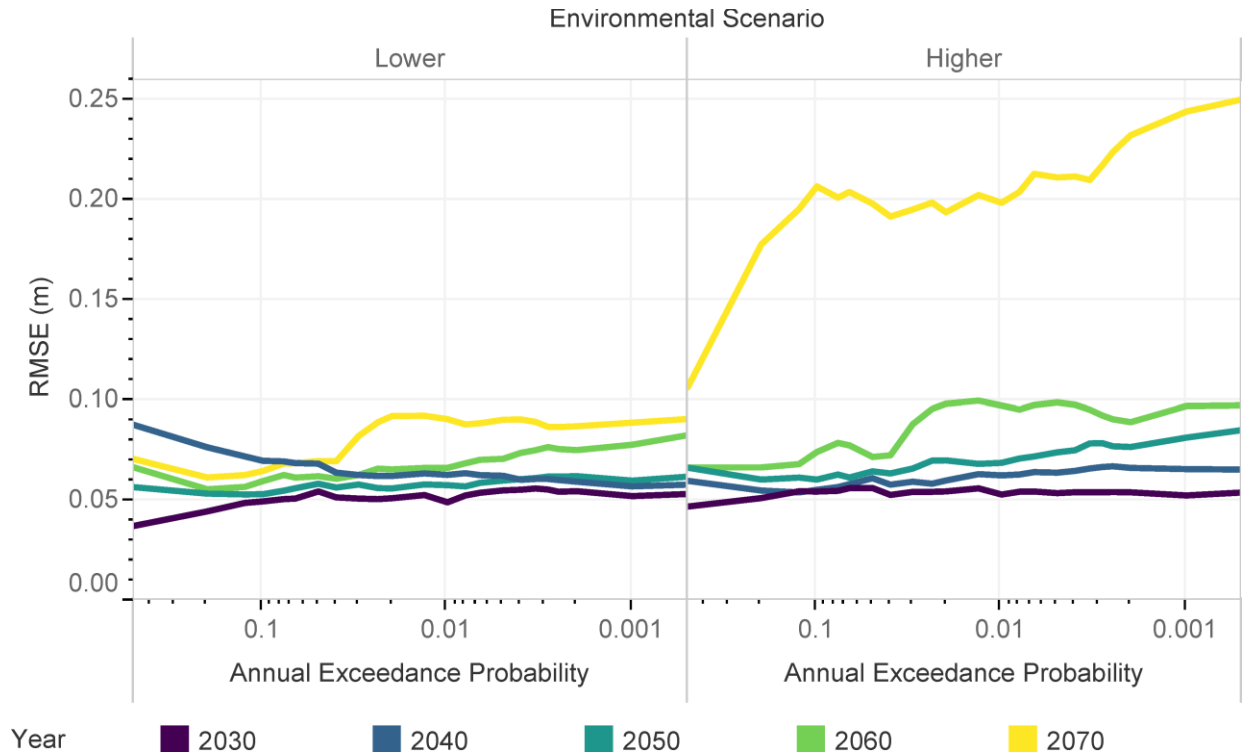


Figure 5. RMSE over all grid points, by annual exceedance probability and landscape.

Considering the full AEP distribution of storm surge at each point and in each landscape, the two-sample Kolmogorov-Smirnov tests further indicate that the surge predictions are accurate enough to usefully inform probabilistic risk studies. In eight of the ten future landscapes, the null hypothesis, that the empirical distributions generated with the ADCIRC simulations and the ANN predictions are drawn from the same underlying probability distribution, is rejected at level $\alpha = 0.05$ for less than one percent of the grid points (Table 1). This table also reports a mean absolute error (MAE) over the grid points below 0.05 m and correlation between simulated and predicted values over 0.99 for all landscapes but the 2070 Higher Scenario.

Table 1. Summary of statistical outcomes for all cases evaluated.

Scenarios	Years	RMSE (m)	MAE (m)	Correlation	Rejected %
Storm-only Model	2020	0.314	0.172	0.912	-
Full Model	2020	0.277	0.077	0.965	-
Higher Scenario	2030	0.063	0.036	0.998	0.76%
	2040	0.069	0.037	0.998	0.69%
	2050	0.076	0.041	0.997	0.56%
	2060	0.082	0.047	0.997	0.40%
	2070	0.206	0.134	0.983	4.84%
Lower Scenario	2030	0.057	0.035	0.998	0.74%
	2040	0.089	0.044	0.996	1.43%
	2050	0.064	0.037	0.998	0.46%
	2060	0.073	0.040	0.997	0.53%
	2070	0.081	0.045	0.997	0.81%

From Table 1, it is evident that by incorporating landscape parameters into the ANN model, storm surge can be predicted accurately for a variety of different scenarios. Figure 6 highlights the spatial pattern of points that rejected the null hypothesis of the two-sided K-S test for an illustrative landscape, the Higher Scenario in 2060. Red points indicate the locations where the test rejects the null hypothesis at $\alpha = 0.05$, while the blue points indicate locations where the evidence fails to rule out the possibility of the hazard estimates coming from the same underlying AEP distribution.

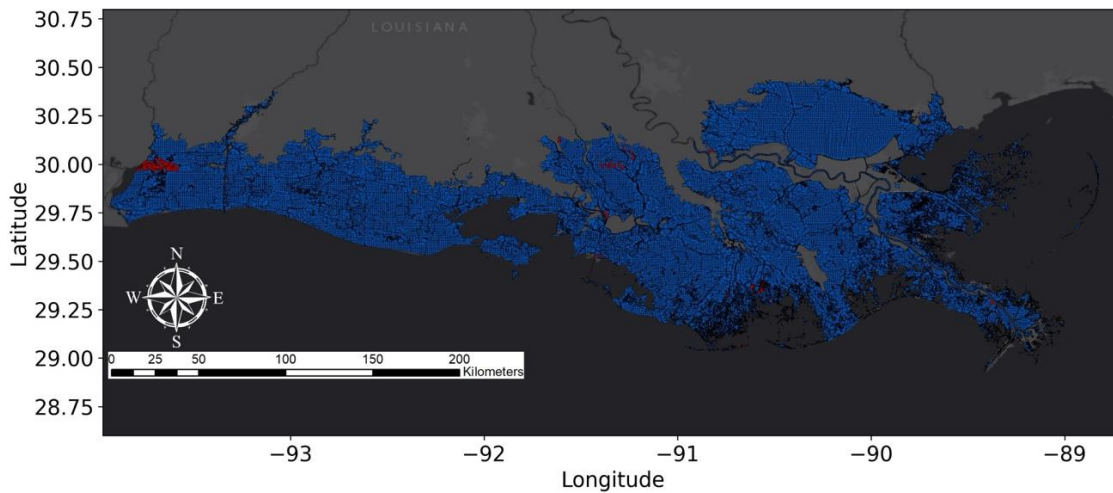


Figure 6. Results of two-sample KS test for the year 2060 of the Higher Scenario. Red indicates points where the null hypothesis is rejected.

Discussion and Conclusions

We have presented a machine learning-based surrogate model of peak storm surge elevations that yields predictions of comparable or greater accuracy, when compared to ADCIRC simulations, than the ADCIRC model relative to historic observations used for model calibration and validation. The addition of future landscapes with variation in landscape parameters and mean sea level conditions provides more features and heterogeneity in training data to improve the model's accuracy. In a leave-one-landscape-out cross-validation exercise, the model produced a mean absolute error of approximately 0.04 m in nine out of ten of the future landscapes, with the exception being the year 2070 of the Higher Scenario, the most extreme landscape with respect to having the greatest sea level rise and land subsidence. A two-sided Kolmogorov-Smirnov test failed to reject the null hypothesis, that points on hazard curves generated by the ADCIRC simulations and ANN predictions are drawn from the same underlying distribution, at less than 1% of grid points in eight out of ten of the future landscapes.

This highlights an important caveat: this analysis utilized ADCIRC simulations that were readily available from Louisiana's 2023 Coastal Master Plan, meaning that the scenarios and time periods were not chosen with the idea of using ADCIRC to train a surrogate model already in mind. This work therefore represents a proof of concept where the ANN model produced predictions suitable for planning studies from a training set of convenience. If planners are interested in estimating risk over a 50-year planning horizon ending in 2070, it may be that accuracy could be improved for the same computational cost by replacing one of the "intermediate" landscapes with a landscape corresponding to the year 2080 instead, to mitigate the challenges of ML models in extrapolating beyond data in their training set.

This also has implications for the storm selection process, given that the 90 storms simulated in each future landscape were chosen by comparing hazard curves to the curve associated with the full 645-storm suite in the current conditions landscape (Fischbach et al., 2021). Prior research has suggested a difficulty in using ML methods to predict extreme storm surge elevations (Hashemi et al., 2016; Ramos-Valle et al., 2021). While accurate reproduction of extreme individual events is important in controlling the overall RMSE and MAE of the model, extreme storms (i.e., with lower central pressures at landfall) are relatively more rare in occurrence, thus having smaller probability masses when contributing to annual exceedance probability distributions and making smaller contributions to expected annual damage calculations.

Consequently, adoption of surrogate models as scenario generators would also benefit from a rigorous consideration of how optimal sampling techniques could be extended to include heterogeneity in landscape parameters and boundary conditions. When planning an analysis that will span a range of future states of the world, it is likely that greater computational efficiency could be achieved by sampling different synthetic storm events on each landscape, rather than simulating the same 90 storms as was done for the Coastal Master Plan.

All the future landscapes used for training our ANN came from the Coastal Master Plan's Future Without Action scenarios (i.e., no additional projects implemented on the landscape). This means we have restricted our predictions to analyzing a slowly evolving landscape without major coastal management interventions. However, the surrogate model developed in this study would also have utility in evaluating the flood risk impacts of coastal restoration projects that affect landscape morphology over time scales ranging from the immediate (e.g., beach nourishment) to decadal (e.g., river diversions).

This study enables better modeling of future climate and environmental conditions by policy makers and water resource managers. Moreover, the developed model makes it possible to evaluate risk under a greater number and range of future scenarios and time periods, opening the door to the use of computationally expensive models like ADCIRC for planning studies utilizing techniques for decision-making under deep uncertainty that require or benefit from the use of large ensembles of future states of the world (Johnson & Geldner, 2019).

Author contributions

David Johnson designed the conceptual framework and analysis plan and led the writing of the paper. Mohammad Ahmadi developed, debugged, and refined the model, executed the analysis, and contributed to writing the paper.

Data and code availability

Model source code, written in Python 3 and R, is available at https://github.com/mohammadahmadi1995/Storm_Surge. Data for this project are available at DesignSafe-CI, <https://doi.org/10.17603/ds2-0ksb-yy40>.

Acknowledgements

This work was supported by the U.S. National Science Foundation under awards 2238060 and 2118329. We thank members of the modeling teams for Louisiana's *Comprehensive Master Plan for a Sustainable Coast* and funding from the Coastal Protection and Restoration Authority for the original simulation data used in this study. Any opinions, findings, conclusions, and recommendations expressed in this material are those of the authors and do not necessarily reflect the views of the funding entities.

References

- Al Kajbaf, A., & Bensi, M. (2020). Application of surrogate models in estimation of storm surge: A comparative assessment. *Applied Soft Computing*, *91*, 106184.
- Bartz-Beielstein, T., & Zaefferer, M. (2017). Model-based methods for continuous and discrete global optimization. *Applied Soft Computing*, *55*, 154–167. <https://doi.org/10.1016/j.asoc.2017.01.039>
- Bates, P. D., Horritt, M. S., & Fewtrell, T. J. (2010). A simple inertial formulation of the shallow water equations for efficient two-dimensional flood inundation modelling. *Journal of Hydrology*, *387*(1–2), 33–45. <https://doi.org/10.1016/j.jhydrol.2010.03.027>
- Bekasiewicz, A., Koziel, S., & Pankiewicz, B. (2015). Accelerated simulation-driven design optimisation of compact couplers by means of two-level space mapping. *IET Microwaves, Antennas & Propagation*, *9*(7), 618–626. <https://doi.org/10.1049/iet-map.2014.0444>
- Chen, W.-B., Liu, W.-C., & Hsu, M.-H. (2012). Predicting typhoon-induced storm surge tide with a two-dimensional hydrodynamic model and artificial neural network model. *Natural Hazards and Earth System Sciences*, *12*(12), 3799–3809. <https://doi.org/10.5194/nhess-12-3799-2012>
- Coastal Protection and Restoration Authority. (2023). *Coastal Master Plan: Appendix B: Scenario Development and Future Conditions* (Version 3; p. 18). Coastal Protection and Restoration Authority. https://coastal.la.gov/wp-content/uploads/2023/01/E1_2023StormSurge_Waves_Report_Jan2021.pdf
- Cobell, Z., & Roberts, H. J. (2021). *Coastal Master Plan: Attachment E1: Storm Surge and Waves Model Improvements* (p. 56). Coastal Protection and Restoration Authority. https://coastal.la.gov/wp-content/uploads/2023/05/B_ScenarioDevelopmentFutureConditions_Jan2023_v3.pdf
- De Oliveira, M. M. F., Ebecken, N. F. F., De Oliveira, J. L. F., & De Azevedo Santos, I. (2009). Neural Network Model to Predict a Storm Surge. *Journal of Applied Meteorology and Climatology*, *48*(1), 143–155. <https://doi.org/10.1175/2008JAMC1907.1>
- Fischbach, J. R., Johnson, D. R., & Kuhn, K. (2016). Bias and efficiency tradeoffs in the selection of storm suites used to estimate flood risk. *Journal of Marine Science and Engineering*, *4*(1), 10.
- Fischbach, J. R., Johnson, D. R., Wilson, M. T., Geldner, N. B., & Stelzner, C. (2021). *2023 Coastal Master Plan: Model Improvement Report, Risk Assessment*. Louisiana Coastal Protection and Restoration Authority.

- Hashemi, M. R., Spaulding, M. L., Shaw, A., Farhadi, H., & Lewis, M. (2016). An efficient artificial intelligence model for prediction of tropical storm surge. *Natural Hazards*, 82(1), 471–491. <https://doi.org/10.1007/s11069-016-2193-4>
- Jammoussi, I., & Ben Nasr, M. (2020). A Hybrid Method Based on Extreme Learning Machine and Self Organizing Map for Pattern Classification. *Computational Intelligence and Neuroscience*, 2020, 1–9. <https://doi.org/10.1155/2020/2918276>
- Jia, G., & Taflanidis, A. A. (2013). Kriging metamodeling for approximation of high-dimensional wave and surge responses in real-time storm/hurricane risk assessment. *Computer Methods in Applied Mechanics and Engineering*, 261–262, 24–38. <https://doi.org/10.1016/j.cma.2013.03.012>
- Jia, G., Taflanidis, A. A., Nadal-Caraballo, N. C., Melby, J. A., Kennedy, A. B., & Smith, J. M. (2015). Surrogate modeling for peak or time-dependent storm surge prediction over an extended coastal region using an existing database of synthetic storms. *Natural Hazards*, 81(2), 909–938. <https://doi.org/10.1007/s11069-015-2111-1>
- Jia, G., Taflanidis, A. A., Nadal-Caraballo, N. C., Melby, J. A., Kennedy, A. B., & Smith, J. M. (2016). Surrogate modeling for peak or time-dependent storm surge prediction over an extended coastal region using an existing database of synthetic storms. *Natural Hazards*, 81(2), 909–938. <https://doi.org/10.1007/s11069-015-2111-1>
- Johnson, D. R., Fischbach, J. R., Geldner, N. B., Wilson, M. T., Story, C., & Wang, J. (2023). *Coastal Master Plan: Attachment C11: 2023 Risk Model* (Version 2; p. 33). Coastal Protection and Restoration Authority. https://coastal.la.gov/wp-content/uploads/2023/04/C11_2023RiskModel_Jan2023_v2.pdf
- Johnson, D. R., Fischbach, J. R., & Ortiz, D. S. (2013). Estimating Surge-Based Flood Risk with the Coastal Louisiana Risk Assessment Model. *Journal of Coastal Research*, 67 (10067), 109–126. https://doi.org/10.2112/SI_67_8
- Johnson, D. R., & Geldner, N. B. (2019). Contemporary decision methods for agricultural, environmental, and resource management and policy. *Annual Review of Resource Economics*, 11, 19–41.
- Kim, S., Pan, S., & Mase, H. (2019). Artificial neural network-based storm surge forecast model: Practical application to Sakai Minato, Japan. *Applied Ocean Research*, 91, 101871. <https://doi.org/10.1016/j.apor.2019.101871>
- Kyprioti, A. P., Taflanidis, A. A., Nadal-Caraballo, N. C., & Campbell, M. O. (2021). Incorporation of sea level rise in storm surge surrogate modeling. *Natural Hazards*, 105(1), 531–563. <https://doi.org/10.1007/s11069-020-04322-z>

- Kyprioti, A. P., Taflanidis, A. A., Nadal-Caraballo, N. C., Yawn, M. C., & Aucoin, L. A. (2022). Integration of Node Classification in Storm Surge Surrogate Modeling. *Journal of Marine Science and Engineering*, 10(4), 551. <https://doi.org/10.3390/jmse10040551>
- Kyprioti, A. P., Taflanidis, A. A., Plumlee, M., Asher, T. G., Spiller, E., Luettich, R. A., Blanton, B., Kijewski-Correa, T. L., Kennedy, A., & Schmied, L. (2021). Improvements in storm surge surrogate modeling for synthetic storm parameterization, node condition classification and implementation to small size databases. *Natural Hazards*, 109(2), 1349–1386. <https://doi.org/10.1007/s11069-021-04881-9>
- Lee, T.-L. (2006). Neural network prediction of a storm surge. *Ocean Engineering*, 33(3–4), 483–494. <https://doi.org/10.1016/j.oceaneng.2005.04.012>
- Lee, T.-L. (2009). Predictions of typhoon storm surge in Taiwan using artificial neural networks. *Advances in Engineering Software*, 40(11), 1200–1206. <https://doi.org/10.1016/j.advengsoft.2007.06.005>
- Mokrech, M., Hanson, S., Nicholls, R. J., Wolf, J., Walkden, M., Fontaine, C. M., Nicholson-Cole, S., Jude, S. R., Leake, J., Stansby, P., Watkinson, A. R., Rounsevell, M. D. A., Lowe, J. A., & Hall, J. W. (2011). The Tyndall coastal simulator. *Journal of Coastal Conservation*, 15(3), 325–335. <https://doi.org/10.1007/s11852-009-0083-6>
- Nadal-Caraballo, N. C., Campbell, M. O., Gonzalez, V. M., Torres, M. J., Melby, J. A., & Taflanidis, A. A. (2020). Coastal hazards system: A probabilistic coastal hazard analysis framework. *Journal of Coastal Research*, 95(SI), 1211–1216.
- Rajasekaran, S., Gayathri, S., & Lee, T.-L. (2008). Support vector regression methodology for storm surge predictions. *Ocean Engineering*, 35(16), 1578–1587. <https://doi.org/10.1016/j.oceaneng.2008.08.004>
- Ramos-Valle, A. N., Curchitser, E. N., Bruyère, C. L., & McOwen, S. (2021). Implementation of an Artificial Neural Network for Storm Surge Forecasting. *Journal of Geophysical Research: Atmospheres*, 126(13). <https://doi.org/10.1029/2020JD033266>
- Reed, D. J., & White, E. D. (2023). *Appendix C: Use of Predictive Models in the 2023 Coastal Master Plan* (Version 3). Coastal Protection and Restoration Authority.
- Resio, D. T. (2007). White paper on estimating hurricane inundation probabilities. In *Performance Evaluation of the New Orleans and Southeast Louisiana Hurricane Protection System. Appendix 8: Hazard Analysis: Vol. VIII*. U.S. Army Corps of Engineers.
- Resio, D. T., Irish, J., & Cialone, M. (2009). A surge response function approach to coastal hazard assessment—part 1: Basic concepts. *Natural Hazards*, 51(1), 163–182.

- Roberts, H. J., & Cobell, Z. (2017). *Coastal Master Plan Modeling: Attachment C3-25.1 – Storm Surge* (p. 110). Coastal Protection and Restoration Authority.
- Shisler, M. P., & Johnson, D. R. (2020). Comparison of Methods for Imputing Non-Wetting Storm Surge to Improve Hazard Characterization. *Water*, 12(5), Article 5. <https://doi.org/10.3390/w12051420>
- Smirnov, N. V. (1939). Estimate of deviation between empirical distribution functions in two independent samples. *Bulletin of Moscow University*, 2(2), 3–16.
- Sztobryn, M. (2003). Forecast of storm surge by means of artificial neural network. *Journal of Sea Research*, 49(4), 317–322. [https://doi.org/10.1016/S1385-1101\(03\)00024-8](https://doi.org/10.1016/S1385-1101(03)00024-8)
- Toro, G. R., Resio, D. T., Divoky, D., Niedoroda, A. W., & Reed, C. (2010). Efficient joint-probability methods for hurricane surge frequency analysis. *Ocean Engineering*, 37(1), 125–134.
- Wamsley, T. V., Cialone, M. A., Smith, J. M., Ebersole, B. A., & Grzegorzewski, A. S. (2009). Influence of landscape restoration and degradation on storm surge and waves in southern Louisiana. *Natural Hazards*, 51(1), 207–224. <https://doi.org/10.1007/s11069-009-9378-z>
- White, E. D., Reed, D. J., & Meselhe, E. A. (2019). Modeled Sediment Availability, Deposition, and Decadal Land Change in Coastal Louisiana Marshes under Future Relative Sea Level Rise Scenarios. *Wetlands*, 39(6), 1233–1248. <https://doi.org/10.1007/s13157-019-01151-0>
- Yang, K., Paramygin, V., & Sheng, Y. P. (2019). An objective and efficient method for estimating probabilistic coastal inundation hazards. *Natural Hazards*, 99(2), 1105–1130. <https://doi.org/10.1007/s11069-019-03807-w>
- Zhang, J., Taflanidis, A. A., Nadal-Caraballo, N. C., Melby, J. A., & Diop, F. (2018). Advances in surrogate modeling for storm surge prediction: Storm selection and addressing characteristics related to climate change. *Natural Hazards*, 94(3), 1225–1253.
- Zhang, K., Liu, H., Li, Y., Xu, H., Shen, J., Rhome, J., & Smith, T. J. (2012). The role of mangroves in attenuating storm surges. *Estuarine, Coastal and Shelf Science*, 102–103, 11–23. <https://doi.org/10.1016/j.ecss.2012.02.021>

Supplementary Information

Table S1. Distribution of synthetic storm parameters at landfall.

Storm ID	Heading	v_f (knots)	r_{max} (nm)	Landfall lon (x)	c_p (mbar)
1	35.8	9.5	10.9	-102.376	865.25
2	35.8	15.3	14.7	-102.375	885.25
3	35.8	11.8	5.9	-102.377	905.25
4	35.8	9.1	9.2	-102.377	925.25
5	35.8	16.7	15.5	-102.378	945.25
6	35.8	8.3	31.3	-102.376	965.25
7	35.8	10.2	59	-102.377	985.25
8	35.8	9.9	23.4	-102.377	1005.25
9	62.72727	20.6	9	-98.8967	865.25
10	62.72727	7.3	5.1	-98.8991	885.25
11	62.72727	8.6	27.3	-98.8964	905.25
12	62.72727	10.2	25.3	-98.8974	925.25
13	62.72727	4.8	27.5	-98.8975	945.25
14	62.72727	9.3	22.4	-98.8986	965.25
15	62.72727	9.7	11.7	-98.899	985.25
16	62.72727	10.9	44.5	-98.899	1005.25
17	69.86364	9.8	5	-95.3612	865.25
18	69.86364	14.4	11.9	-95.3631	885.25
19	69.86364	5.1	16.4	-95.36	905.25
20	69.86364	17.2	10.2	-95.359	925.25
21	69.86364	7.8	36.8	-95.3605	945.25
22	69.86364	9.8	25.1	-95.3612	965.25
23	69.86364	4.6	9	-95.3626	985.25
24	69.86364	12.3	56.6	-95.3634	1005.25
25	69.88333	10.9	6	-91.8512	865.25
26	69.88333	5.2	8	-91.85	885.25
27	69.88333	10.5	19.8	-91.85	905.25
28	69.88333	6.7	42.3	-91.8499	925.25
29	69.88333	17.5	26.5	-91.8528	945.25
30	69.88333	8.6	11.4	-91.8494	965.25

31	69.88333	11.8	51.2	-91.8525	985.25
32	69.88333	5.2	35.9	-91.8503	1005.25
33	77.34848	11.2	7.7	-88.3561	865.25
34	77.34848	18.1	15.7	-88.3545	885.25
35	77.34848	11.4	17.9	-88.3557	905.25
36	77.34848	8.5	11.8	-88.3535	925.25
37	77.34848	9.3	49.6	-88.3521	945.25
38	77.34848	5	27.1	-88.3541	965.25
39	77.34848	4.5	19	-88.3534	985.25
40	77.34848	13.2	33.4	-88.355	1005.25
41	88.96364	6.3	8.8	-85.1718	865.25
42	89.01786	11.3	6.3	-85.1751	885.25
43	88.96364	13.2	29	-85.1714	905.25
44	88.96364	8	34.8	-85.1727	925.25
45	88.96364	6.2	17.6	-85.1724	945.25
46	88.96364	17	23.3	-85.1735	965.25
47	88.96364	8.5	21.9	-85.1722	985.25
48	88.96364	7.7	62.4	-85.1726	1005.25
49	48.39024	9.6	17.7	-96.13	875.25
50	48.39024	15.9	16.4	-96.1307	895.25
51	48.39024	8.7	8.9	-96.1314	915.25
52	48.39024	9.6	9.3	-96.13	935.25
53	48.39024	16.8	13	-96.1303	955.25
54	48.39024	11.5	50.9	-96.131	975.25
55	48.39024	4.8	32.6	-96.1309	995.25
56	49.06522	21.9	13.9	-94.9388	875.25
57	49.06522	14.9	9.4	-94.9391	895.25
58	49.06522	9.3	7.6	-94.9392	915.25
59	49.06522	10.5	22.4	-94.9383	935.25
60	49.06522	5.3	16	-94.9385	955.25
61	49.06522	11.9	48.7	-94.9389	975.25
62	49.06522	12	15	-94.9388	995.25
63	51.03846	24.4	7.6	-93.7258	875.25
64	51.03846	13.2	9.7	-93.7262	895.25
65	51.03846	5.5	19.4	-93.7253	915.25
66	51.03846	8	44.4	-93.7255	935.25

67	51.03846	8.3	9.2	-93.7247	955.25
68	51.03846	12.6	35.9	-93.7253	975.25
69	51.03846	8.4	28	-93.725	995.25
70	51.05172	5.3	13.4	-92.5434	875.25
71	51.05172	17.5	11.8	-92.5442	895.25
72	51.05172	9.6	9.7	-92.5436	915.25
73	51.05172	4.9	15.4	-92.5437	935.25
74	51.05172	5.8	27	-92.5433	955.25
75	51.05172	9.8	44.8	-92.5445	975.25
76	51.05172	6	11.2	-92.5439	995.25
77	52.05085	13.6	11.2	-91.324	875.25
78	52.05085	9.2	13.2	-91.325	895.25
79	52.05085	14.5	20.7	-91.3244	915.25
80	52.05085	9.3	48	-91.3253	935.25
81	52.05085	9.6	12.2	-91.3248	955.25
82	52.05085	6.2	28.8	-91.324	975.25
83	52.05085	15	47	-91.3246	995.25
84	54.83051	6.8	13	-90.1105	875.25
85	54.83051	15.4	12.9	-90.1105	895.25
86	54.83051	12.5	14.4	-90.1102	915.25
87	54.83051	9.1	41.7	-90.11	935.25
88	54.83051	13.6	22.5	-90.1105	955.25
89	54.83051	5.6	20	-90.1113	975.25
90	54.83051	11	55.5	-90.1107	995.25
91	57.39063	8.3	7.8	-88.9005	875.25
92	57.39063	9.4	7.2	-88.9003	895.25
93	57.39063	8.2	27.6	-88.9001	915.25
94	57.39063	13.2	14.8	-88.9003	935.25
95	57.39063	9.9	51.2	-88.9006	955.25
96	58.02985	10.9	14.6	-88.9	975.25
97	58.02985	5.1	37.7	-88.8991	995.25
98	60.03077	9.9	9.6	-87.7248	875.25
99	60.03077	5.7	18.7	-87.7257	895.25
100	60.03077	6.9	13.4	-87.7242	915.25
101	60.03077	15	10.5	-87.7249	935.25
102	60.03077	12.7	59.2	-87.7245	955.25

103	60.03077	12.2	33.4	-87.7247	975.25
104	60.03077	8.9	33.8	-87.7245	995.25
105	66.86667	12.7	15	-86.4704	875.25
106	66.86667	11.4	6.6	-86.4712	895.25
107	66.86667	5.8	18.2	-86.4713	915.25
108	66.86667	14.5	11.7	-86.4705	935.25
109	66.86667	10.7	54.6	-86.4709	955.25
110	66.86667	13.4	23.7	-86.4713	975.25
111	66.86667	9.3	69.1	-86.4709	995.25
112	69.01786	8.6	6.4	-85.25	875.25
113	69.01786	10.7	20.1	-85.2502	895.25
114	69.01786	9	10.6	-85.2499	915.25
115	69.01786	16	13.6	-85.25	935.25
116	69.01786	5.6	19.1	-85.251	955.25
117	69.01786	9.2	68.6	-85.2507	975.25
118	69.01786	7.3	22.8	-85.2501	995.25
119	29.62791	7.9	9.2	-95.5716	865.25
120	29.62791	21.2	9.8	-95.5717	885.25
121	29.62791	13.7	8	-95.5719	905.25
122	29.62791	9.9	33.2	-95.5718	925.25
123	29.62791	6.9	18.4	-95.5716	945.25
124	29.62791	15.6	9	-95.5719	965.25
125	29.62791	9.2	36.3	-95.5716	985.25
126	29.62791	4.6	15.4	-95.5718	1005.25
127	29.06522	8.5	5.6	-94.7963	865.25
128	29.06522	23.7	16.8	-94.7964	885.25
129	29.06522	8.1	10.7	-94.7971	905.25
130	29.06522	11.8	6.6	-94.7967	925.25
131	29.06522	19.4	32.8	-94.7964	945.25
132	29.06522	5.5	40.4	-94.7961	965.25
133	29.06522	10.8	26	-94.7964	985.25
134	29.06522	4.3	12.6	-94.7964	1005.25
135	28.97959	16.2	6.2	-94.0161	865.25
136	28.97959	16.3	5.6	-94.016	885.25
137	28.97959	15.4	11.4	-94.0157	905.25
138	28.97959	8.3	29.2	-94.0159	925.25

139	28.97959	5.7	35.4	-94.0148	945.25
140	28.97959	4.9	13	-94.0158	965.25
141	28.97959	15.7	31.4	-94.0163	985.25
142	28.97959	9	14.5	-94.0163	1005.25
143	30.55172	23.7	4.6	-93.2425	865.25
144	30.55172	18.7	10.1	-93.2417	885.25
145	30.55172	6.7	9.9	-93.2419	905.25
146	30.55172	14.5	26.2	-93.242	925.25
147	30.55172	10.8	9.4	-93.2426	945.25
148	30.55172	6.7	47.6	-93.2425	965.25
149	30.55172	5	30.3	-93.2418	985.25
150	30.55172	9.2	20.4	-93.2424	1005.25
151	30.48276	27	12.7	-92.4729	865.25
152	30.48276	12.4	7.5	-92.4726	885.25
153	30.48276	6.2	19.2	-92.4723	905.25
154	30.48276	8.8	12.3	-92.4727	925.25
155	30.48276	18.4	8	-92.4726	945.25
156	30.48276	13.1	38.9	-92.4725	965.25
157	30.48276	11.4	21	-92.4725	985.25
158	30.48276	7.9	40	-92.4724	1005.25
159	30.15	19.8	5.9	-91.6849	865.25
160	30.15	16.8	20.2	-91.6852	885.25
161	30.15	21	9.2	-91.685	905.25
162	30.15	7.2	13.9	-91.6848	925.25
163	30.15	14.5	7.4	-91.6843	945.25
164	30.15	5.9	37.5	-91.6849	965.25
165	30.15	13.3	35	-91.6848	985.25
166	30.15	7.3	10.7	-91.6844	1005.25
167	34.58333	13.9	13.3	-90.8992	865.25
168	34.58333	9.1	5.3	-90.899	885.25
169	34.58333	5.6	14.4	-90.8989	905.25
170	34.58333	15.4	23.6	-90.8992	925.25
171	34.58333	6.4	29.5	-90.8993	945.25
172	34.58333	9.1	32.5	-90.899	965.25
173	34.58333	11.1	72.2	-90.8988	985.25
174	34.58333	8.5	16.4	-90.8984	1005.25

175	34.83051	9.2	6.8	-90.1173	865.25
176	34.83051	9.4	13.8	-90.1173	885.25
177	34.83051	14.5	14	-90.117	905.25
178	34.83051	7.7	39.1	-90.1168	925.25
179	34.83051	15	14.8	-90.1171	945.25
180	34.83051	19.3	29.2	-90.1171	965.25
181	34.83051	9.4	27	-90.1167	985.25
182	34.83051	9.7	59.3	-90.1174	1005.25
183	35.16129	11.9	9.5	-89.3274	865.25
184	35.16129	13.2	15.1	-89.3277	885.25
185	35.16129	7.5	7.7	-89.327	905.25
186	35.16129	5.9	27.1	-89.3273	925.25
187	35.16129	15.5	22.2	-89.3271	945.25
188	35.16129	10.4	64.3	-89.3273	965.25
189	35.16129	17.7	12.6	-89.3277	985.25
190	35.16129	6.4	54.2	-89.3281	1005.25
191	37.71014	12.3	11.7	-88.543	865.25
192	37.71014	7.6	17.5	-88.5434	885.25
193	37.71014	16.5	13.6	-88.5435	905.25
194	37.71014	13.2	7.7	-88.5424	925.25
195	37.71014	7.6	19.1	-88.5434	945.25
196	37.71014	8.1	59.3	-88.5433	965.25
197	37.71014	15	24.9	-88.5434	985.25
198	37.71014	11.5	48.1	-88.5431	1005.25
199	40.03077	8.2	6.6	-87.7427	865.25
200	40.03077	17.4	7.2	-87.7434	885.25
201	40.03077	12.1	16.8	-87.7433	905.25
202	40.03077	9.3	8.2	-87.7439	925.25
203	40.03077	12.1	34.1	-87.743	945.25
204	40.03077	5.2	16.3	-87.7433	965.25
205	40.03077	9.9	66.6	-87.743	985.25
206	40.03077	10.3	32.2	-87.7432	1005.25
207	43.95082	6.6	5.5	-86.9481	865.25
208	43.95082	11.7	11.6	-86.9488	885.25
209	43.95082	14	7.3	-86.9486	905.25
210	43.95082	5.7	31.7	-86.9491	925.25

211	43.95082	9.9	30.5	-86.9481	945.25
212	43.95082	11.6	36.2	-86.9482	965.25
213	43.95082	6.4	15.3	-86.9487	985.25
214	43.95082	15.2	18.4	-86.9481	1005.25
215	47.26667	13.5	8.2	-86.1468	865.25
216	47.26667	5.5	9	-86.1468	885.25
217	47.26667	10.8	7	-86.1458	905.25
218	47.26667	12.5	21.3	-86.147	925.25
219	47.26667	8	44.1	-86.1462	945.25
220	47.26667	13.5	18	-86.1468	965.25
221	47.26667	7.2	42.1	-86.1464	985.25
222	47.26667	6	13.5	-86.1458	1005.25
223	9.627907	18.6	8	-95.6178	875.25
224	9.627907	9.8	10.4	-95.6183	895.25
225	9.627907	17.1	20	-95.6178	915.25
226	9.627907	5.3	35.9	-95.6178	935.25
227	9.627907	15.5	7.8	-95.6181	955.25
228	9.627907	5.1	17.2	-95.6176	975.25
229	9.627907	10.7	58.1	-95.6175	995.25
230	9.065217	15.3	6.6	-94.9837	875.25
231	9.065217	5.2	19.3	-94.9838	895.25
232	9.065217	11.1	6.3	-94.9839	915.25
233	9.065217	20.1	9.9	-94.9838	935.25
234	9.065217	12	31.2	-94.9831	955.25
235	9.065217	7.4	27.8	-94.9835	975.25
236	9.065217	7	18.8	-94.9836	995.25
237	9.469388	15.8	15.7	-94.3494	875.25
238	9.469388	6.9	10.7	-94.349	895.25
239	9.469388	18.5	17.1	-94.3493	915.25
240	9.469388	12.9	8.2	-94.3491	935.25
241	9.469388	18.7	20.8	-94.3494	955.25
242	9.469388	6.4	56.1	-94.349	975.25
243	9.469388	6.2	26.9	-94.3489	995.25
244	11.03846	17.3	10.6	-93.7128	875.25
245	11.03846	14	5.5	-93.7131	895.25
246	11.03846	6	15.9	-93.7127	915.25

247	11.03846	18.1	12.3	-93.7127	935.25
248	11.03846	10.2	28	-93.7128	955.25
249	11.03846	8.1	18.1	-93.713	975.25
250	11.03846	7.6	50.9	-93.7131	995.25
251	11.24138	23	7	-93.0786	875.25
252	11.24138	11.8	12.1	-93.0777	895.25
253	11.24138	15	34	-93.0781	915.25
254	11.24138	6.3	7.6	-93.0782	935.25
255	11.24138	5.1	21.6	-93.0782	955.25
256	11.24138	10.6	20.9	-93.0784	975.25
257	11.24138	11.3	35.1	-93.0782	995.25
258	10.48276	7.4	8.4	-92.4393	875.25
259	10.48276	18.9	8.2	-92.4392	895.25
260	10.48276	21.5	28.9	-92.4393	915.25
261	10.48276	10.8	17.4	-92.4393	935.25
262	10.48276	4.7	18.4	-92.4391	955.25
263	10.48276	11.2	38.6	-92.4391	975.25
264	10.48276	5.3	9.3	-92.4389	995.25
265	10.10169	11	11.5	-91.7978	875.25
266	10.10169	6	7.6	-91.7972	895.25
267	10.10169	5	26.5	-91.797	915.25
268	10.10169	10.2	29.5	-91.797	935.25
269	10.10169	7.8	10	-91.7975	955.25
270	10.10169	8.5	22.8	-91.7972	975.25
271	10.10169	4.9	42	-91.7972	995.25
272	12.82759	14.8	11.8	-91.1511	875.25
273	12.82759	13.6	14.9	-91.1512	895.25
274	12.82759	7.9	14.9	-91.1508	915.25
275	12.82759	5.6	28.5	-91.151	935.25
276	12.82759	10.4	46.1	-91.151	955.25
277	12.82759	7.6	26.7	-91.1507	975.25
278	12.82759	17	31.4	-91.151	995.25
279	12.50909	10.3	4.9	-90.515	875.25
280	10.10169	8	17.4	-91.7973	895.25
281	10.10169	15.9	36.6	-91.7974	915.25
282	10.10169	6.5	21.6	-91.7977	935.25

283	10.10169	17.7	16.7	-91.7975	955.25
284	10.10169	14.4	21.8	-91.7973	975.25
285	10.10169	9.8	43.6	-91.7971	995.25
286	14.77193	16.3	7.3	-89.869	875.25
287	14.77193	8.6	8.5	-89.8692	895.25
288	14.77193	5.3	25.5	-89.8691	915.25
289	14.77193	8.8	23.9	-89.8695	935.25
290	14.77193	11.3	44	-89.869	955.25
291	14.77193	8.3	16.4	-89.8694	975.25
292	14.77193	13.2	53.1	-89.8689	995.25
293	16.70313	10.6	9.1	-89.2264	875.25
294	16.70313	12.9	7.9	-89.2268	895.25
295	16.70313	17.8	16.5	-89.2269	915.25
296	16.70313	5.8	19.4	-89.2265	935.25
297	16.70313	6.7	40.4	-89.227	955.25
298	16.70313	15	37.1	-89.2265	975.25
299	16.70313	6.8	15.9	-89.2262	995.25
300	17.71014	5.9	16.6	-88.5732	875.25
301	17.71014	16.4	12.5	-88.5734	895.25
302	17.71014	10.2	8.4	-88.5733	915.25
303	17.71014	9.9	13	-88.5729	935.25
304	17.71014	6.5	23.3	-88.573	955.25
305	17.71014	13	59.3	-88.5727	975.25
306	17.71014	10.1	17.8	-88.5729	995.25
307	20.14925	14.4	5.2	-87.9329	875.25
308	20.14925	8.3	21.9	-87.9333	895.25
309	20.14925	15.4	15.4	-87.9336	915.25
310	20.14925	19	33	-87.933	935.25
311	20.14925	7.4	10.7	-87.9331	955.25
312	20.14925	7.2	31	-87.9329	975.25
313	20.14925	15.9	24.8	-87.9332	995.25
314	23.04762	7.1	5.6	-87.2823	875.25
315	23.04762	17	15.4	-87.2825	895.25
316	23.04762	7.6	22.9	-87.2822	915.25
317	23.04762	17.3	25.6	-87.2828	935.25
318	23.04762	8.9	14.5	-87.2822	955.25

319	23.04762	10	63.3	-87.2824	975.25
320	23.04762	10.4	30.3	-87.2825	995.25
321	23.73438	13.9	8.2	-86.6288	875.25
322	23.73438	7.7	14.5	-86.6291	895.25
323	23.73438	9.9	11.6	-86.6295	915.25
324	23.73438	12.1	39.5	-86.6291	935.25
325	23.73438	7.6	29	-86.6289	955.25
326	23.73438	5.7	41.5	-86.6292	975.25
327	23.73438	12.4	14	-86.6289	995.25
328	-10.3721	5.4	7	-95.54	865.25
329	-10.3721	19.5	8.5	-95.54	885.25
330	-10.3721	9.2	6.2	-95.54	905.25
331	-10.3721	9.6	30.4	-95.54	925.25
332	-10.3721	12.8	23.1	-95.54	945.25
333	-10.3721	8.8	15.4	-95.54	965.25
334	-10.3721	7.8	37.7	-95.54	985.25
335	-10.3721	5	21.3	-95.54	1005.25
336	-10.9348	10.5	11.3	-94.93	865.25
337	-10.9348	22.3	6	-94.93	885.25
338	-10.9348	23.9	15.8	-94.93	905.25
339	-10.9348	13.7	22.1	-94.93	925.25
340	-10.9348	7.3	12.7	-94.93	945.25
341	-10.9348	5.7	43.7	-94.93	965.25
342	-10.9348	8.3	22.9	-94.93	985.25
343	-10.9348	6.2	27.6	-94.93	1005.25
344	-10.5306	15.7	7.1	-94.32	865.25
345	-10.5306	20.3	11	-94.32	885.25
346	-10.5306	19.1	8.4	-94.32	905.25
347	-10.5306	11.1	36.7	-94.32	925.25
348	-10.5306	9.1	11.4	-94.32	945.25
349	-10.5306	14.4	33.6	-94.32	965.25
350	-10.5306	4.9	32.6	-94.32	985.25
351	-10.5306	9.4	25.5	-94.32	1005.25
352	-8.96154	21.5	4.3	-93.71	865.25
353	-8.96154	6.7	10.4	-93.71	885.25
354	-8.96154	12.9	10.3	-93.71	905.25

355	-8.96154	19.7	15.6	-93.71	925.25
356	-8.96154	9.6	13.4	-93.71	945.25
357	-8.96154	7.2	52.5	-93.71	965.25
358	-8.96154	8.7	40.6	-93.71	985.25
359	-8.96154	6.6	17.4	-93.71	1005.25
360	-8.75862	19.1	9.7	-93.1	865.25
361	-8.75862	25.4	7	-93.1	885.25
362	-8.75862	20	17.4	-93.1	905.25
363	-8.75862	5.5	11.2	-93.1	925.25
364	-8.75862	8.3	40	-93.1	945.25
365	-8.75862	6.3	30.2	-93.1	965.25
366	-8.75862	6.6	9.8	-93.1	985.25
367	-8.75862	11.2	31	-93.1	1005.25
368	-9.51724	7	7.3	-92.49	865.25
369	-9.51724	14.8	6.7	-92.49	885.25
370	-9.51724	17.7	22	-92.49	905.25
371	-9.51724	20.8	14.5	-92.49	925.25
372	-9.51724	11.1	31.6	-92.49	945.25
373	-9.51724	7.6	19.7	-92.49	965.25
374	-9.51724	5.2	49.1	-92.49	985.25
375	-9.51724	5.5	9.7	-92.49	1005.25
376	-9.77966	17.8	12.1	-91.88	865.25
377	-9.77966	12.8	8.3	-91.88	885.25
378	-9.77966	5.3	22.8	-91.88	905.25
379	-9.77966	17.9	7.1	-91.88	925.25
380	-9.77966	11.4	21.4	-91.88	945.25
381	-9.77966	4.6	10.6	-91.88	965.25
382	-9.77966	5.8	43.6	-91.88	985.25
383	-9.77966	8.7	34.6	-91.88	1005.25
384	-7.50877	17.2	10.6	-91.27	865.25
385	-7.50877	8.7	13.4	-91.27	885.25
386	-7.50877	7.2	11.1	-91.27	905.25
387	-7.50877	12.9	12.9	-91.27	925.25
388	-7.50877	10.2	46.5	-91.27	945.25
389	-7.50877	13.9	26.1	-91.27	965.25
390	-7.50877	7.6	18.1	-91.27	985.25

391	-7.50877	8.1	41.5	-91.27	1005.25
392	-6.81356	8.9	4.5	-90.66	865.25
393	-6.81356	10.7	21.7	-90.66	885.25
394	-6.81356	5.9	25.9	-90.66	905.25
395	-6.81356	11.4	18.6	-90.66	925.25
396	-6.81356	5.9	24.7	-90.66	945.25
397	-6.81356	11.3	18.8	-90.66	965.25
398	-6.81356	7	10.7	-90.66	985.25
399	-6.81356	8.3	70.5	-90.66	1005.25
400	-5.22807	13.1	7.5	-90.05	865.25
401	-5.22807	14	10.7	-90.05	885.25
402	-5.22807	18.4	23.8	-90.05	905.25
403	-5.22807	10.8	10.7	-90.05	925.25
404	-5.22807	5.2	16.9	-90.05	945.25
405	-5.22807	7.4	28.1	-90.05	965.25
406	-5.22807	9	62.4	-90.05	985.25
407	-5.22807	13.7	26.5	-90.05	1005.25
408	-2.91667	12.7	4.9	-89.44	865.25
409	-2.91667	8.2	18.3	-89.44	885.25
410	-2.91667	6.4	9.5	-89.44	905.25
411	-2.91667	15	16.8	-89.44	925.25
412	-2.91667	12.4	8.7	-89.44	945.25
413	-2.91667	11.9	49.9	-89.44	965.25
414	-2.91667	13.8	17.2	-89.44	985.25
415	-2.91667	5.7	46.3	-89.44	1005.25
416	-2.02899	5.7	4.8	-88.83	865.25
417	-2.02899	10	9.6	-88.83	885.25
418	-2.02899	10.2	31.3	-88.83	905.25
419	-2.02899	14	24.4	-88.83	925.25
420	-2.02899	5.5	25.6	-88.83	945.25
421	-2.02899	7.9	9.8	-88.83	965.25
422	-2.02899	6	39.1	-88.83	985.25
423	-2.02899	12.7	49.9	-88.83	1005.25
424	-1.38235	14.7	8	-88.22	865.25
425	-1.38235	5.8	12.3	-88.22	885.25
426	-1.38235	12.5	13.1	-88.22	905.25

427	-1.38235	9.1	15.1	-88.22	925.25
428	-1.38235	10.5	16.2	-88.22	945.25
429	-1.38235	15	34.9	-88.22	965.25
430	-1.38235	8	53.5	-88.22	985.25
431	-1.38235	7	22.4	-88.22	1005.25
432	0.030769	7.6	5.7	-87.61	865.25
433	0.030769	15.8	7.7	-87.61	885.25
434	0.030769	9	20.5	-87.61	905.25
435	0.030769	16	16.2	-87.61	925.25
436	0.030769	13.2	12	-87.61	945.25
437	0.030769	16.2	55.6	-87.61	965.25
438	0.030769	10.5	28.1	-87.61	985.25
439	0.030769	6.7	38.6	-87.61	1005.25
440	3.746032	10.2	14.2	-87	865.25
441	3.746032	8.5	5.8	-87	885.25
442	3.746032	15	12.3	-87	905.25
443	3.746032	18.7	19.3	-87	925.25
444	3.746032	8.6	19.9	-87	945.25
445	3.746032	6.5	21.4	-87	965.25
446	3.746032	12.1	56	-87	985.25
447	3.746032	10.5	19.3	-87	1005.25
448	-30.3721	16.8	6.7	-95.6029	875.25
449	-30.3721	5.5	21	-95.6032	895.25
450	-30.3721	10.5	6.7	-95.6027	915.25
451	-30.3721	21.6	11.1	-95.6035	935.25
452	-30.3721	12.4	33.5	-95.603	955.25
453	-30.3721	7.8	29.9	-95.6029	975.25
454	-30.3721	7.2	19.8	-95.6029	995.25
455	-30.9348	12	5.5	-94.9587	875.25
456	-30.9348	10.4	5.8	-94.9584	895.25
457	-30.9348	11.4	23.7	-94.9587	915.25
458	-30.9348	15.5	16.1	-94.9584	935.25
459	-30.9348	8.6	24.2	-94.9584	955.25
460	-30.9348	6.7	8.6	-94.9586	975.25
461	-30.9348	4.4	21.8	-94.9581	995.25
462	-30.5306	12.4	5.8	-94.3234	875.25

463	-30.5306	12.1	6	-94.3233	895.25
464	-30.5306	11.8	24.6	-94.3235	915.25
465	-30.5306	16.6	16.7	-94.3231	935.25
466	-30.5306	9.1	26.1	-94.3232	955.25
467	-30.5306	7	9.4	-94.3238	975.25
468	-30.5306	4.6	23.8	-94.3233	995.25
469	-28.9615	8	8.9	-93.6883	875.25
470	-28.9615	20.6	8.8	-93.6879	895.25
471	-28.9615	19.3	30.3	-93.6881	915.25
472	-28.9615	11.4	18.7	-93.6883	935.25
473	-28.9615	4.9	19.9	-93.6881	955.25
474	-28.9615	9	40	-93.6876	975.25
475	-28.9615	5.5	10.3	-93.6877	995.25
476	-28.7586	6.2	9.8	-93.0572	875.25
477	-28.7586	24.7	13.7	-93.0568	895.25
478	-28.7586	13.7	7.1	-93.0573	915.25
479	-28.7586	8.5	30.6	-93.0574	935.25
480	-28.7586	13.1	15.2	-93.0567	955.25
481	-28.7586	4.5	13.7	-93.0577	975.25
482	-28.7586	8	45.2	-93.0571	995.25
483	-29.5172	9	4.7	-92.4166	875.25
484	-29.5172	7.4	26.2	-92.4166	895.25
485	-29.5172	23.1	17.6	-92.4166	915.25
486	-29.5172	7	27.5	-92.4167	935.25
487	-29.5172	6	11.4	-92.4168	955.25
488	-29.5172	15.6	12	-92.4165	975.25
489	-29.5172	8.6	74.8	-92.4166	995.25
490	-29.8983	11.7	10.1	-91.7894	875.25
491	-29.8983	19.7	11.4	-91.7894	895.25
492	-29.8983	7.1	8	-91.7895	915.25
493	-29.8983	6	18	-91.7897	935.25
494	-29.8983	11.7	36	-91.7894	955.25
495	-29.8983	16.4	12.9	-91.7894	975.25
496	-29.8983	7.8	61.1	-91.7894	995.25
497	-27.1724	6.5	12.5	-91.1497	875.25
498	-27.1724	18.2	9.1	-91.1499	895.25

499	-27.1724	20.4	31.9	-91.15	915.25
500	-27.1724	8.3	26.6	-91.1502	935.25
501	-27.1724	8.1	8.5	-91.1499	955.25
502	-27.1724	5	34.6	-91.1502	975.25
503	-27.1724	11.6	39.1	-91.1499	995.25
504	-27.4909	17.9	9.3	-90.5184	875.25
505	-27.4909	6.3	15.9	-90.5178	895.25
506	-27.4909	12.1	18.8	-90.5182	915.25
507	-27.4909	7.8	8.7	-90.5185	935.25
508	-27.4909	9.3	38.8	-90.5184	955.25
509	-27.4909	4.8	24.7	-90.5184	975.25
510	-27.4909	13.8	36.4	-90.5181	995.25
511	-25.2281	5.6	7.2	-89.8916	875.25
512	-25.2281	11.1	16.9	-89.8916	895.25
513	-25.2281	10.8	11.1	-89.8916	915.25
514	-25.2281	13.6	20.8	-89.8916	935.25
515	-25.2281	14	17.5	-89.8916	955.25
516	-25.2281	8.7	53.3	-89.8917	975.25
517	-25.2281	5.7	25.9	-89.8917	995.25
518	-23.2969	9.3	8.6	-89.26	875.25
519	-23.2969	6.6	24.4	-89.2601	895.25
520	-23.2969	6.6	12.5	-89.2601	915.25
521	-23.2969	12.5	31.7	-89.26	935.25
522	-23.2969	16.1	13.7	-89.2602	955.25
523	-23.2969	10.3	25.7	-89.2597	975.25
524	-23.2969	6.4	40.5	-89.2599	995.25
525	-22.3971	7.7	6	-88.6229	875.25
526	-22.3971	10.1	10	-88.623	895.25
527	-22.3971	8.4	22.1	-88.6226	915.25
528	-22.3971	7.3	37.5	-88.6226	935.25
529	-22.3971	15	25.1	-88.6229	955.25
530	-22.3971	9.5	11.1	-88.6229	975.25
531	-22.3971	5.8	48.9	-88.6228	995.25
532	-19.8507	11.3	10.9	-87.9992	875.25
533	-19.8507	12.5	11.1	-87.9995	895.25
534	-19.8507	14	9.3	-87.9994	915.25

535	-19.8507	6.8	34.4	-87.9992	935.25
536	-19.8507	20	30.1	-87.9993	955.25
537	-19.8507	5.3	19.1	-87.999	975.25
538	-19.8507	12.8	29.2	-87.9994	995.25
539	-17.5	19.3	10.3	-87.3666	875.25
540	-17.5	7.1	14	-87.3669	895.25
541	-17.5	13.2	12	-87.3672	915.25
542	-17.5	11.1	23.1	-87.3669	935.25
543	-17.5	7.1	32.3	-87.3669	955.25
544	-17.5	18.5	43.1	-87.3673	975.25
545	-17.5	8.2	13.1	-87.3671	995.25
546	-49.6939	22.5	5.2	-94.1419	865.25
547	-49.6939	7.9	13	-94.1421	885.25
548	-49.6939	9.8	12.7	-94.1424	905.25
549	-49.6939	22.4	20	-94.1412	925.25
550	-49.6939	8.9	53.7	-94.1425	945.25
551	-49.6939	10.1	8.2	-94.1423	965.25
552	-49.6939	5.4	16.2	-94.1432	985.25
553	-49.6939	10	37.2	-94.1426	1005.25
554	-49.4483	6	7.8	-93.3481	865.25
555	-49.4483	11	12.6	-93.3489	885.25
556	-49.4483	22.2	18.5	-93.3481	905.25
557	-49.4483	6.4	18	-93.3482	925.25
558	-49.4483	13.6	10.7	-93.348	945.25
559	-49.4483	18	12.2	-93.3483	965.25
560	-49.4483	6.8	29.2	-93.3481	985.25
561	-49.4483	7.5	76.3	-93.3485	1005.25
562	-48.9483	14.3	8.4	-92.5574	865.25
563	-48.9483	13.6	6.5	-92.5576	885.25
564	-48.9483	17	24.8	-92.5572	905.25
565	-48.9483	6.2	20.6	-92.5577	925.25
566	-48.9483	20.8	23.9	-92.5573	945.25
567	-48.9483	10.7	14.6	-92.5574	965.25
568	-48.9483	6.2	14.4	-92.5577	985.25
569	-48.9483	4.5	52	-92.5578	1005.25
570	-49.8983	25.1	10	-91.7639	865.25

571	-49.8983	9.7	11.3	-91.7647	885.25
572	-49.8983	11.1	6.6	-91.7654	905.25
573	-49.8983	5.2	28.1	-91.7642	925.25
574	-49.8983	5	14.1	-91.7649	945.25
575	-49.8983	12.7	17.1	-91.7652	965.25
576	-49.8983	14.4	45.4	-91.7643	985.25
577	-49.8983	5.9	28.7	-91.7641	1005.25
578	-45.3509	7.2	6.5	-90.9759	865.25
579	-45.3509	6.1	16.2	-90.9762	885.25
580	-45.3509	9.6	11.9	-90.9762	905.25
581	-45.3509	16.6	22.8	-90.976	925.25
582	-45.3509	11.7	10	-90.9763	945.25
583	-45.3509	9.6	45.6	-90.9762	965.25
584	-45.3509	7.4	23.9	-90.9758	985.25
585	-45.3509	11.9	24.4	-90.9763	1005.25
586	-45.1695	16.7	5.3	-90.1883	865.25
587	-45.1695	6.4	19.2	-90.188	885.25
588	-45.1695	8.4	8.8	-90.1883	905.25
589	-45.1695	10.5	17.4	-90.1882	925.25
590	-45.1695	16.1	28.5	-90.1877	945.25
591	-45.1695	7	24.2	-90.1884	965.25
592	-45.1695	16.6	47.1	-90.1883	985.25
593	-45.1695	14.4	11.6	-90.1884	1005.25
594	-42.9167	15.2	8.6	-89.4177	865.25
595	-42.9167	12	8.7	-89.4178	885.25
596	-42.9167	7	21.2	-89.4181	905.25
597	-42.9167	7	8.7	-89.4181	925.25
598	-42.9167	6.6	20.6	-89.418	945.25
599	-42.9167	11	42	-89.418	965.25
600	-42.9167	12.5	20	-89.4176	985.25
601	-42.9167	7.1	29.9	-89.4179	1005.25
602	-42.3971	18.4	10.3	-88.6134	865.25
603	-42.3971	7	9.3	-88.6128	885.25
604	-42.3971	7.8	15.3	-88.6131	905.25
605	-42.3971	7.5	13.4	-88.6129	925.25
606	-42.3971	14	41.9	-88.613	945.25

607	-42.3971	12.3	13.8	-88.6135	965.25
608	-42.3971	12.9	33.8	-88.6133	985.25
609	-42.3971	4.8	43	-88.6134	1005.25
610	-40.9375	11.6	6.4	-87.8442	865.25
611	-40.9375	10.4	14.2	-87.8443	885.25
612	-40.9375	15.9	14.9	-87.8442	905.25
613	-40.9375	12.1	9.7	-87.8445	925.25
614	-40.9375	7.1	38.3	-87.8444	945.25
615	-40.9375	6.1	20.6	-87.8444	965.25
616	-40.9375	5.6	13.4	-87.8444	985.25
617	-40.9375	16.2	66	-87.8445	1005.25
618	-69.5172	20	12.2	-92.4188	875.25
619	-69.5172	14.5	6.4	-92.419	895.25
620	-69.5172	6.3	21.4	-92.4192	915.25
621	-69.5172	11.8	20.1	-92.4196	935.25
622	-69.5172	11	48.4	-92.4191	955.25
623	-69.5172	5.9	10.3	-92.4184	975.25
624	-69.5172	14.4	20.7	-92.4193	995.25
625	-67.5088	13.1	6.2	-91.1804	875.25
626	-67.5088	21.7	18	-91.1802	895.25
627	-67.5088	16.5	10.2	-91.1806	915.25
628	-67.5088	5.1	24.8	-91.18	935.25
629	-67.5088	6.9	42.1	-91.1807	955.25
630	-67.5088	13.9	32.2	-91.1807	975.25
631	-67.5088	6.6	12.1	-91.1807	995.25
632	-65.2281	26.2	5.1	-89.9662	875.25
633	-65.2281	8.9	23.1	-89.9663	895.25
634	-65.2281	12.9	13	-89.9661	915.25
635	-65.2281	14	7	-89.9665	935.25
636	-65.2281	14.4	34.7	-89.9657	955.25
637	-65.2281	6.6	15.4	-89.9659	975.25
638	-65.2281	9.1	64.7	-89.9671	995.25
639	-62.029	20.9	14.4	-88.7649	875.25
640	-62.029	22.9	7	-88.7646	895.25
641	-62.029	7.3	13.9	-88.7656	915.25
642	-62.029	7.5	14.1	-88.766	935.25

643	-62.029	6.3	37.4	-88.765	955.25
644	-62.029	17.3	46.7	-88.7657	975.25
645	-62.029	9.6	16.8	-88.7653	995.25